

SLAC-PUB-578
April 1969
(EXPI)

SWITCHING PROPERTIES OF THE EMITTER-COUPLED TRANSISTOR-PAIR*

Arpad Barna

Stanford Linear Accelerator Center
Stanford University, Stanford, California 94305

ABSTRACT

Switching properties of the emitter-coupled transistor-pair are analyzed by means of a digital computer. Waveforms and risetimes are computed for a wide range of parameters. The resulting risetimes are interpreted in terms of the gain-bandwidth products of the transistors, external capacitances, and the risetime of the input signal.

(Submitted to the 1969 IEEE International Symposium on Circuit Theory.)

*Work supported by the U.S. Atomic Energy Commission.

I. INTRODUCTION

The emitter-coupled transistor pair of Fig. 1 has found many uses in high-speed switching circuits. When components are suitably chosen, the transistors do not saturate and switching times in the nanosecond region are readily attainable. There are many variations of the circuit: Both bases may be driven, one of the two collector resistors, R_{C1} or R_{C2} , may be omitted, current source Q_3 may be replaced by a resistor.

In the following it will be assumed that the circuit of Fig. 2 provides a reasonable approximation to the actual circuit. Transistors Q_1 and Q_2 are characterized by a single fixed parameter $\tau_0 \triangleq 1/(2\pi f_{\tau})$ where f_{τ} is the gain-bandwidth product of both transistors, ohmic base resistances are included in R_g , and all capacitances are lumped into C_{ext} . This approximation is reasonably good if one has the circuit of Fig. 1 with $R_{C1} = 0$: In this case R_{C1} of Fig. 2 is chosen zero and the stray capacitance on the base of Q_1 and its collector-to-base capacitance are included in C_{ext} .

II. COMPUTATION OF THE TRANSIENT

The collector current $i_{C1}(t)$ will be computed for the generator voltage signal $v_g(t)$ of Fig. 3. The hybrid equivalent circuit of Fig. 4 will be used for each transistor with $\alpha \approx 1$, i.e., $\beta \rightarrow \infty$. With these assumptions the circuit shown in Fig. 5 results. It can be seen that the circuit enclosed in the box of broken lines is grounded only via R_B , hence the value and location of R_B is arbitrary; in the following an $R_B = \infty$ will be taken. Also, observing the nodes at B_1 and B_2 it is apparent that all of i_{B1} flows into C_{e1} and all of i_{B2} into C_{e2} . Thus, Fig. 5 can be redrawn as Fig. 6 where C_{ext} has been included in C_{e1} and C_{e2} .

Now, the transient of the circuit can be computed solely from the loop of v_g , R_g , C_{e1} and C_{e2} .

Defining

$$v_{B1E} \stackrel{\Delta}{=} v_{B1} - v_E \quad (1)$$

and

$$v_{B2E} \stackrel{\Delta}{=} v_{B2} - v_E \quad (2)$$

the collector currents are given by the diode equations as

$$i_{C1} = I_0(e^{v_{B1E}/V_T} - 1) \quad (3)$$

and

$$i_{C2} = I_0(e^{v_{B2E}/V_T} - 1), \quad (4)$$

where

$$i_{C1} + i_{C2} = I_{DC}. \quad (5)$$

Here I_0 is the saturation current (in the vicinity of nanoamperes); $V_T = n \frac{kT}{q}$,

where k is the Boltzmann constant $k = 1.38 \times 10^{-23} \text{Ws}/\text{K}$, T is the absolute

temperature in ^0K , and q is the charge of the electron $q = 1.6 \times 10^{-19} \text{As}$.

Constant n is dimensionless, $n \approx 1$ to 1.5 for germanium, $n \approx 1.5$ to 2 for silicon diodes.

The value of kT/q at room temperature is $\approx 25 \text{ mV}$, thus V_T is typically between 25 mV and 50 mV .

Capacitances C_{e1} and C_{e2} are given by

$$C_{e1} \stackrel{\Delta}{=} \frac{dq_{B1E}}{dv_{B1E}} = \frac{d(i_{C1}\tau_0)}{dv_{B1E}} = \frac{\tau_0}{V_T} I_0 e^{v_{B1E}/V_T} \quad (6)$$

and

$$C_{e2} \stackrel{\Delta}{=} \frac{dq_{B2E}}{dv_{B2E}} = \frac{d(i_{C2}\tau_0)}{dv_{B2E}} = \frac{\tau_0}{V_T} I_0 e^{v_{B2E}/V_T}. \quad (7)$$

Also

$$C_{e1}' = C_{e1} + C_{ext} \frac{C_{e1} + C_{e2}}{C_{e2}}, \quad (8)$$

$$C_{e2}' = C_{e2} + C_{ext} \frac{C_{e1} + C_{e2}}{C_{e1}}, \quad (9)$$

and

$$i_{B1} = \frac{v_g + v_{B2E} - v_{B1E}}{R_g}. \quad (10)$$

The base-emitter voltages are given by the integrals

$$v_{B1E} = \int \frac{i_{B1}}{C_{e1}} dt \quad (11)$$

and

$$v_{B2E} = \int \frac{i_{B2}}{C_{e2}} dt = - \int \frac{i_{B1}}{C_{e2}} dt. \quad (12)$$

Unfortunately i_{B1} , C_{e1} , and C_{e2} vary with time and the integrals have to be evaluated numerically. Equation (11) can be approximated as

$$v_{B1E} = \int \frac{i_{B1}}{C_{e1}} dt \approx \sum \frac{i_{B1}}{C_{e1}} \Delta t,$$

which can be also written as

$$v_{B1E}(t + \Delta t) \approx v_{B1E}(t) + \Delta v_1, \quad (13)$$

where

$$\Delta v_1 \triangleq \frac{i_{B1}(t)}{C_{e1}(t)} \Delta t. \quad (14)$$

Similarly (12) becomes

$$v_{B2E}(t + \Delta t) \approx v_{B2E}(t) + \Delta v_2, \quad (15)$$

with

$$\Delta v_2 \triangleq \frac{-i_{B1}(t)}{C_{e2}(t)} \Delta t. \quad (16)$$

The initial values of v_{B1E} and v_{B2E} can be computed from (3), (4), and (5) as

$$v_{B1E}(t = 0) = v_g(t < 0) + V_T \ln \frac{2 + I_{DC}/I_0}{1 + e^{v_g(t < 0)/V_T}} \quad (17)$$

$$v_{B2E}(t = 0) = V_T \ln \frac{2 + I_{DC}/I_0}{1 + e^{v_g(t < 0)/V_T}} \quad (18)$$

and i_{C1} can be computed by substituting (17) into (3).

Equations (3), (8), (9), (10), (13), and (15) are solved by a digital computer using the flow chart of Fig. 7 with $\Delta t_{\max} = 0.01 \tau_0$, $\Delta t_{\min} = 10^{-5} \tau_0$, and $\Delta v_{\max} = 0.01 V_T$.

III. RESULTS

Representative waveforms of $i_{C1}(t)$ are shown in Fig. 8 and Fig. 9.¹ The risetimes between the 10% and 90% points of i_{C1}/I_{DC} are summarized in Table 1, together with those obtained from the approximation

$$t_r \approx \sqrt{(t_{r\tau} + t_{rc})^2 + t_{rg}^2}, \quad (19)$$

where

$$t_{r\tau} \triangleq 0.8 \frac{R_g I_{DC}}{v_{g1} - 0.4 V_T} \tau_0, \quad (20)$$

$$t_{rc} \triangleq \frac{V_T^2 \ln 9}{v_{g1} - 0.8 V_T} R_g C_{ext}, \quad (21)$$

and

$$t_{rg} \triangleq \frac{V_T^2 \ln 9}{v_{g1} - v_{g0}} t_g. \quad (22)$$

There are three contributions to the risetime: 1), $t_{r\tau}$ of (20) results from a finite τ_0 (finite gain - bandwidth product), 2), t_{rc} of (21) results from the finite C_{ext} , and 3), t_{rg} of (22) from the finite risetime t_g of the input signal.

1), t_{RT} . In the limiting case when C_{ext} and t_g are zero, the risetime is given by (20). For $v_{g1} \gg V_T$ this is the current gain $R_g I_{DC} / v_{g1}$ multiplied by τ_0 and by a factor of 0.8 for a risetime computed between 10% and 90%. The term $0.4 V_T \approx 20 \text{ mV}$ in the denominator of (20) represents a voltage "used up" for dc switching, which has to be taken account if $v_{g1} \gg V_T$.

2), t_{rc} . In addition to the charge $I_{DC} \tau_0$ in the base emitter junction, the source has to provide a charge into capacitor C_{ext} which results in the risetime t_{rc} of (21). The dc voltage swing on the bases between the 10% and 90% points of i_{C1} (from (3), (4), and (5) with $i_{C1} \gg I_0$ and $i_{C2} \gg I_0$) is $\approx V_T 2 \ln 9$. Assuming a voltage of 0.8 V_T "lost" from v_{g1} for dc current transfer, t_{rc} represents the charge supplied to C_{ext} during a voltage swing of $V_T^2 \ln 9$.

3), t_{rg} . Equation (22) represents the risetime of the input waveform during the voltage swing of $V_T^2 \ln 9$. Since this risetime t_{rg} is independent of that of the circuit, $t_{RT} + t_{rc}$, the squares of the two risetimes are added in (19).

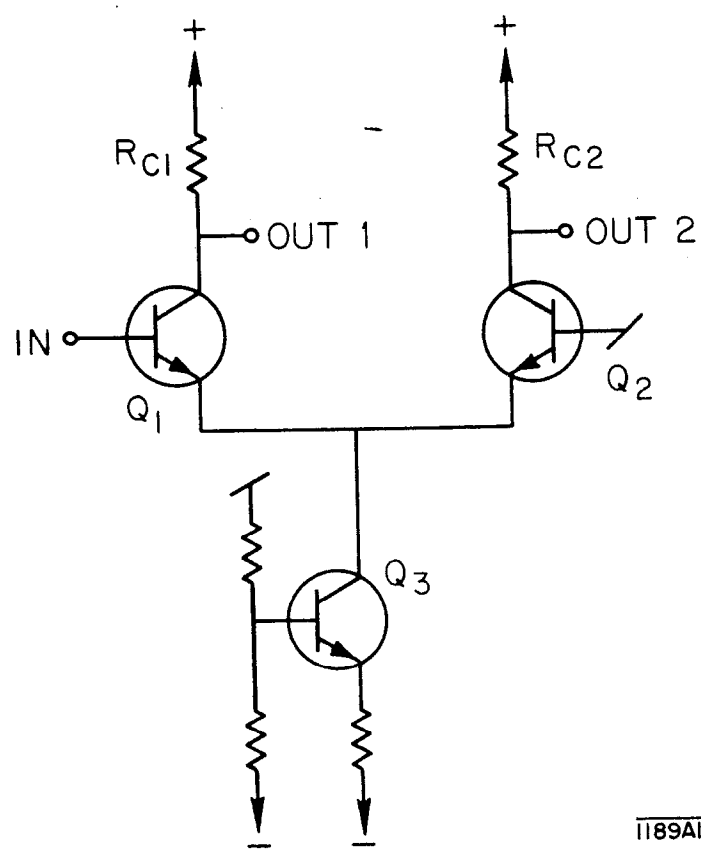
As can be seen in Table 1, Eq. (19) provides a rather good approximation, therefore it can be utilized to obtain risetimes for parameter values not listed in the table.

REFERENCE

1. More detailed results and Fortran-IV programs are available in A. Barna, "High-speed switching properties of the emitter-coupled transistor-pair," Report No. SLAC-97, Stanford Linear Accelerator Center, Stanford University, Stanford, California (March 1969).

FIGURE CAPTIONS

1. Emitter-coupled transistor pair.
2. An approximation of the emitter-coupled transistor pair of Fig. 1.
3. Generator voltage for Fig. 2.
4. Hybrid transistor equivalent circuit.
5. The circuit of Fig. 2 with the transistor equivalent circuit of Fig. 4.
6. Simplification of the circuit of Fig. 5.
- 7a and 7b. Flow-charts of the computer program.
- 8a through 8d. Waveforms of $i_{C1}(t)$ for $C_{ext} = 0$ and various values of v_{g0} ,
 v_{g1} , R_g , and t_g .
- 9a through 9d. Waveforms of $i_{C1}(t)$ for $t_g = 0$ and various values of v_{g0} ,
 v_{g1} , R_g , and C_{ext} .



1189AI

Fig. 1

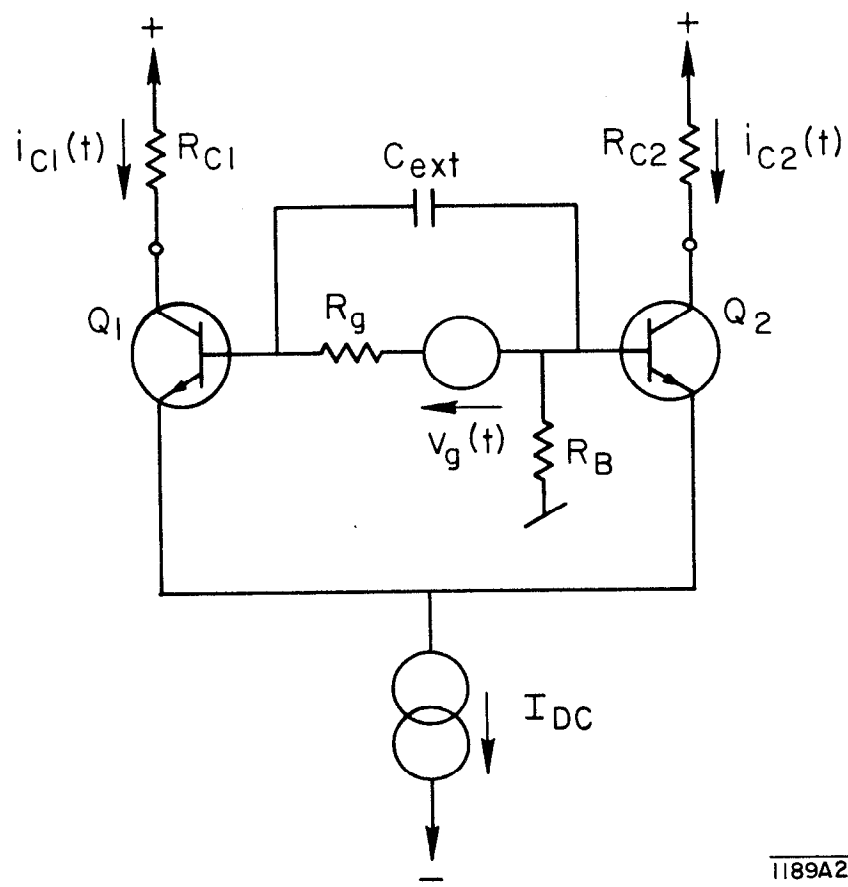
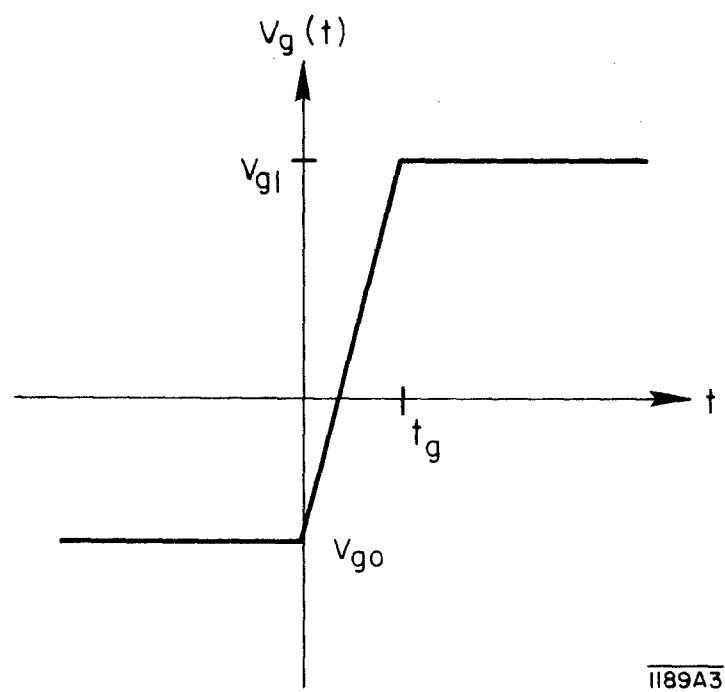


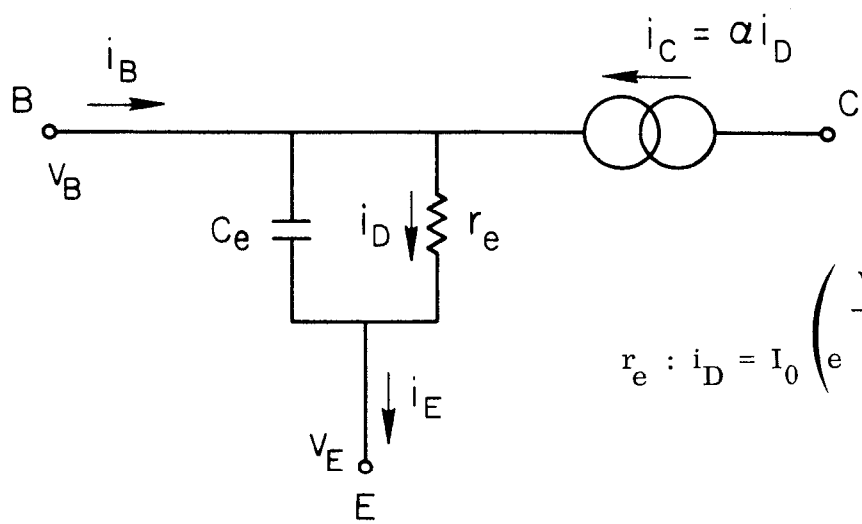
Fig. 2

1189A2



1189A3

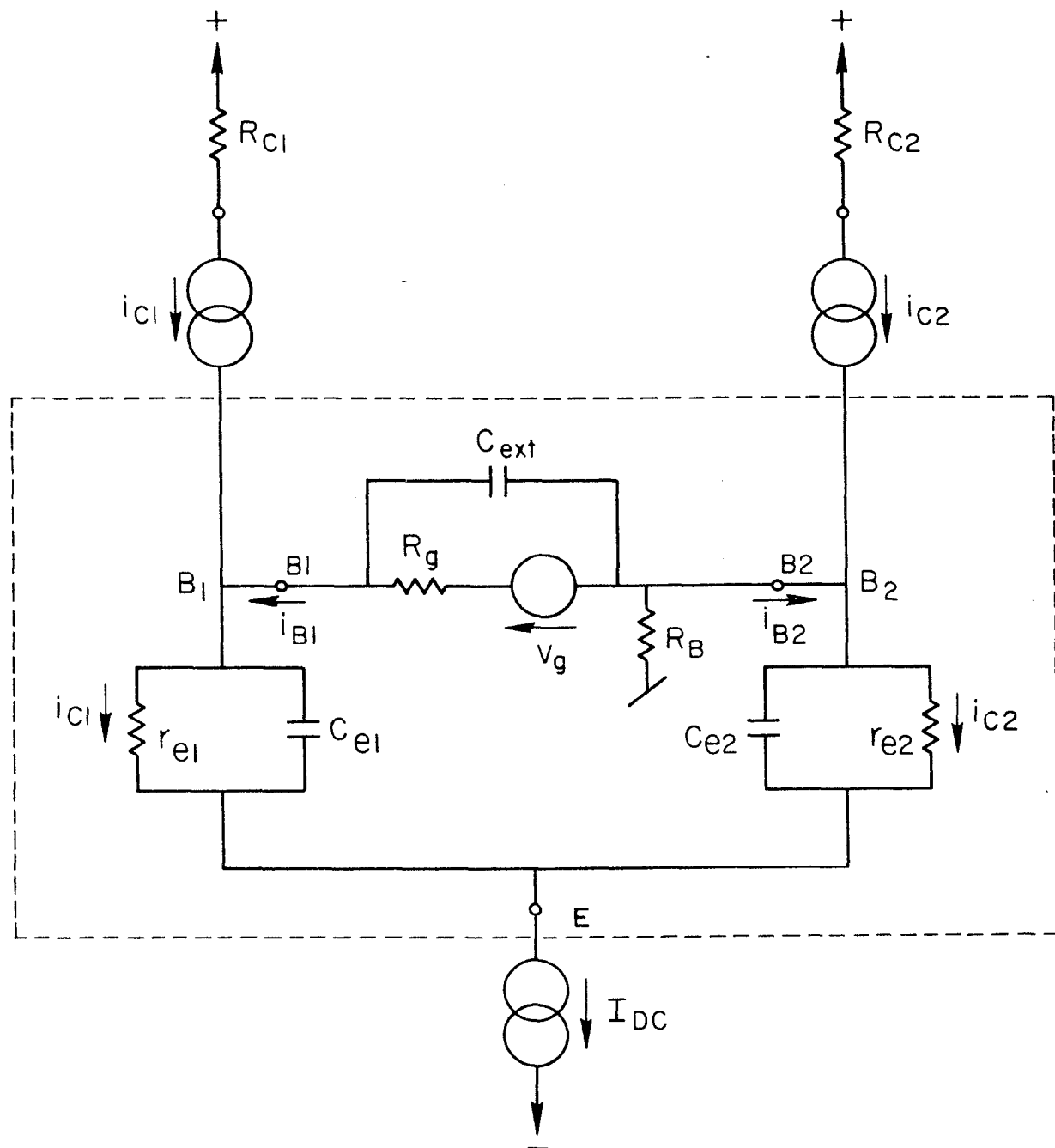
Fig. 3



$$r_e : i_D = I_0 \left(e^{\frac{V_B - V_E}{V_T}} - 1 \right)$$

1189A4

Fig. 4

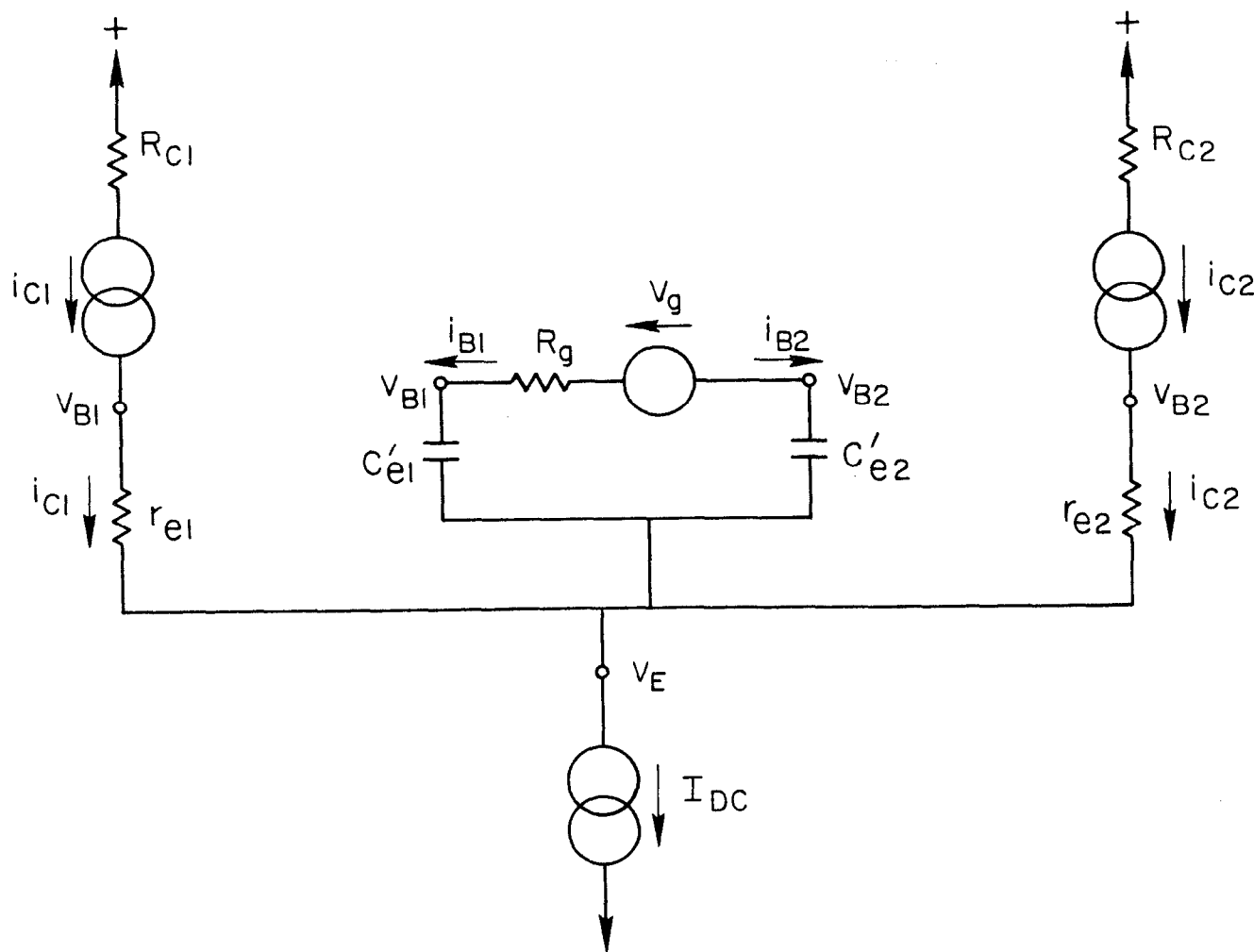


$$r_{e1} : i_{C1} = I_0 \left(e^{\frac{v_{B1} - v_E}{V_T}} - 1 \right)$$

$$r_{e2} : i_{C2} = I_0 \left(e^{\frac{v_{B2} - v_E}{V_T}} - 1 \right)$$

1189A5

Fig. 5



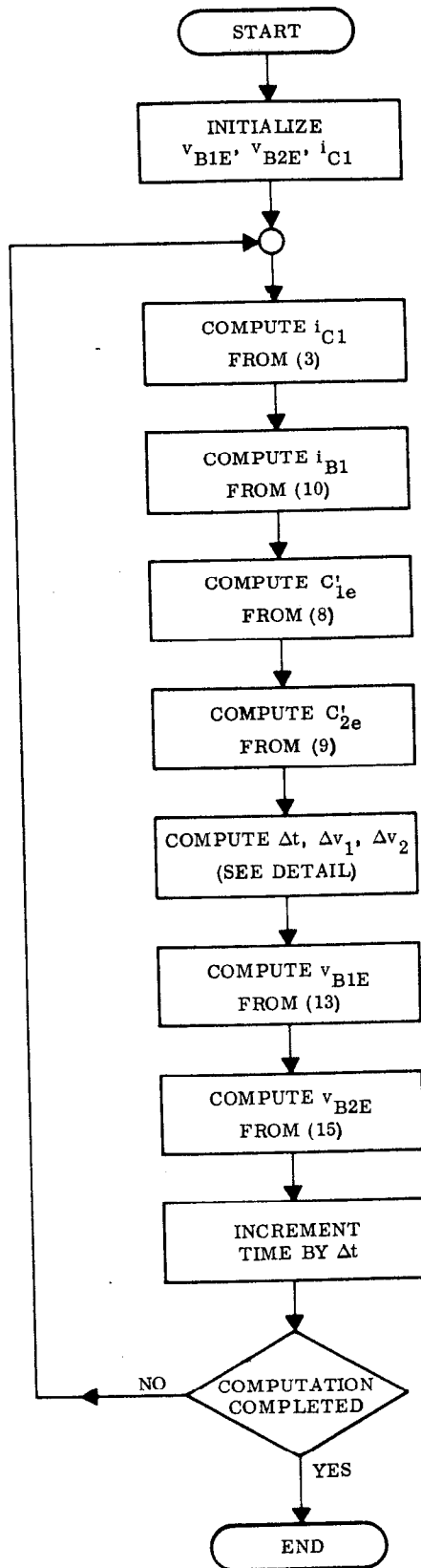
$$r_{e1} : i_{C1} = I_0 \left(e^{\frac{v_{B1} - v_E}{V_T}} - 1 \right) \quad r_{e2} : i_{C2} = I_0 \left(e^{\frac{v_{B2} - v_E}{V_T}} - 1 \right)$$

$$C'_{e1} = C_{e1} + C_{ext} \frac{C_{e1} + C_{e2}}{C_{e2}}$$

$$C'_{e2} = C_{e2} + C_{ext} \frac{C_{e1} + C_{e2}}{C_{e1}}$$

1189A6

Fig. 6



1189A7

Fig. 7a

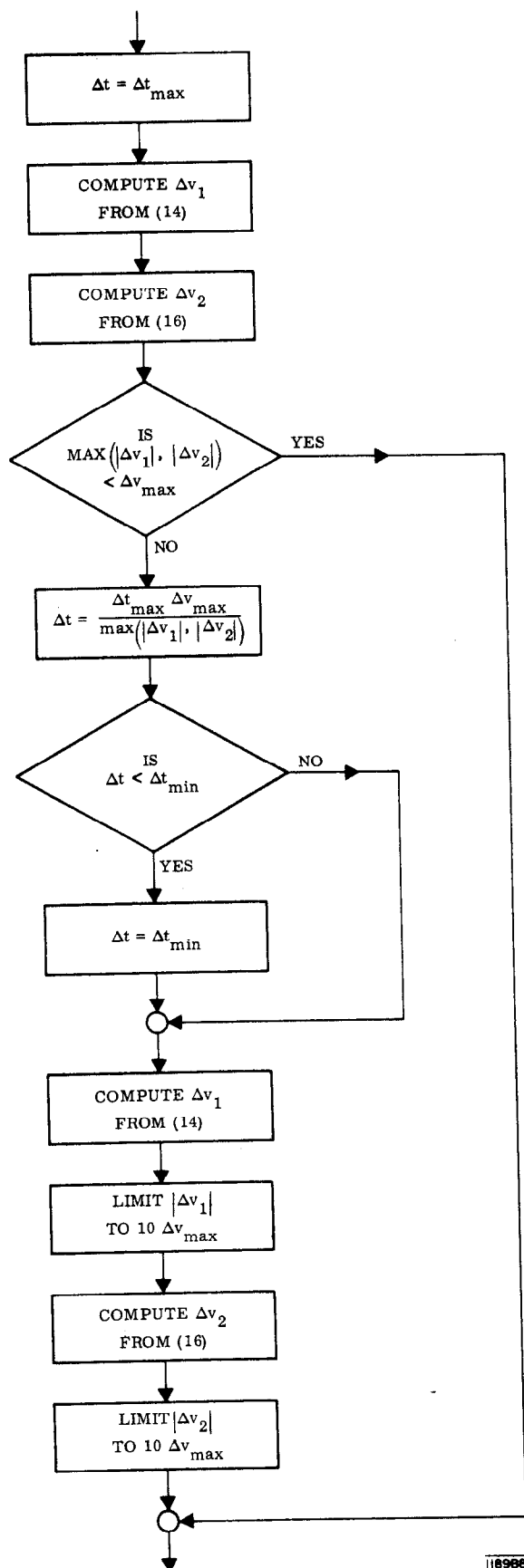


Fig. 7b

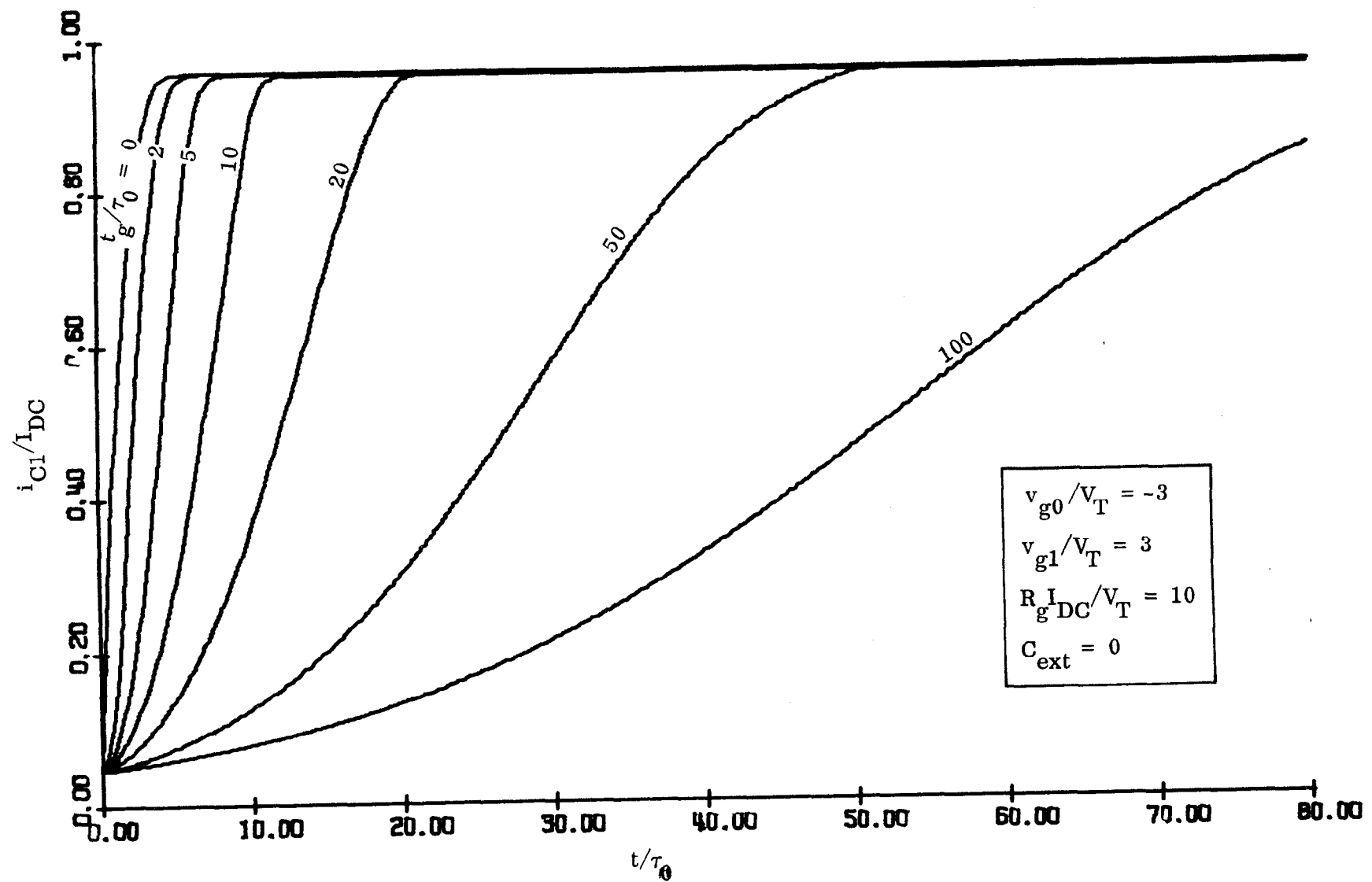


Fig. 8 a

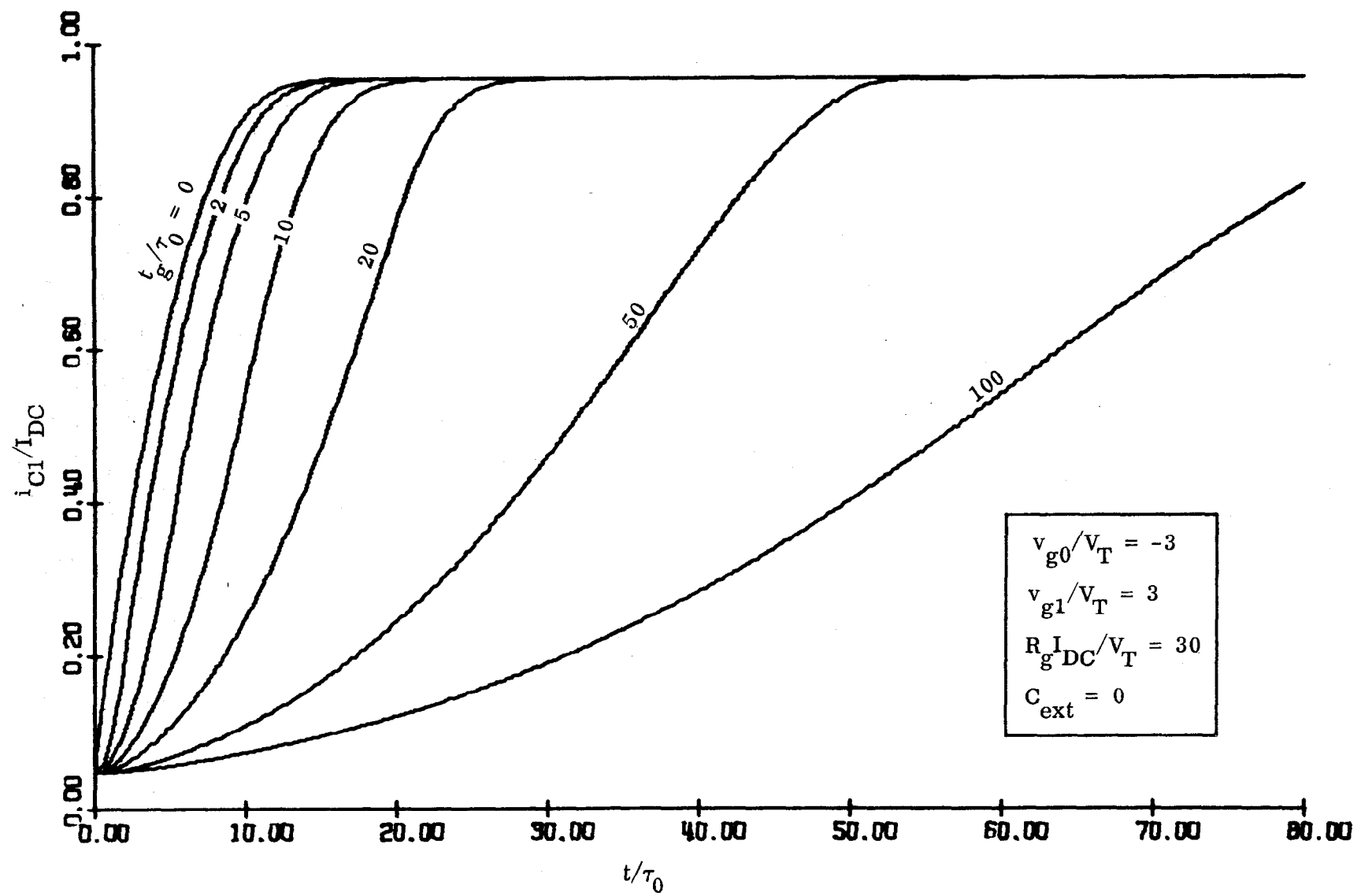


Fig. 8 b

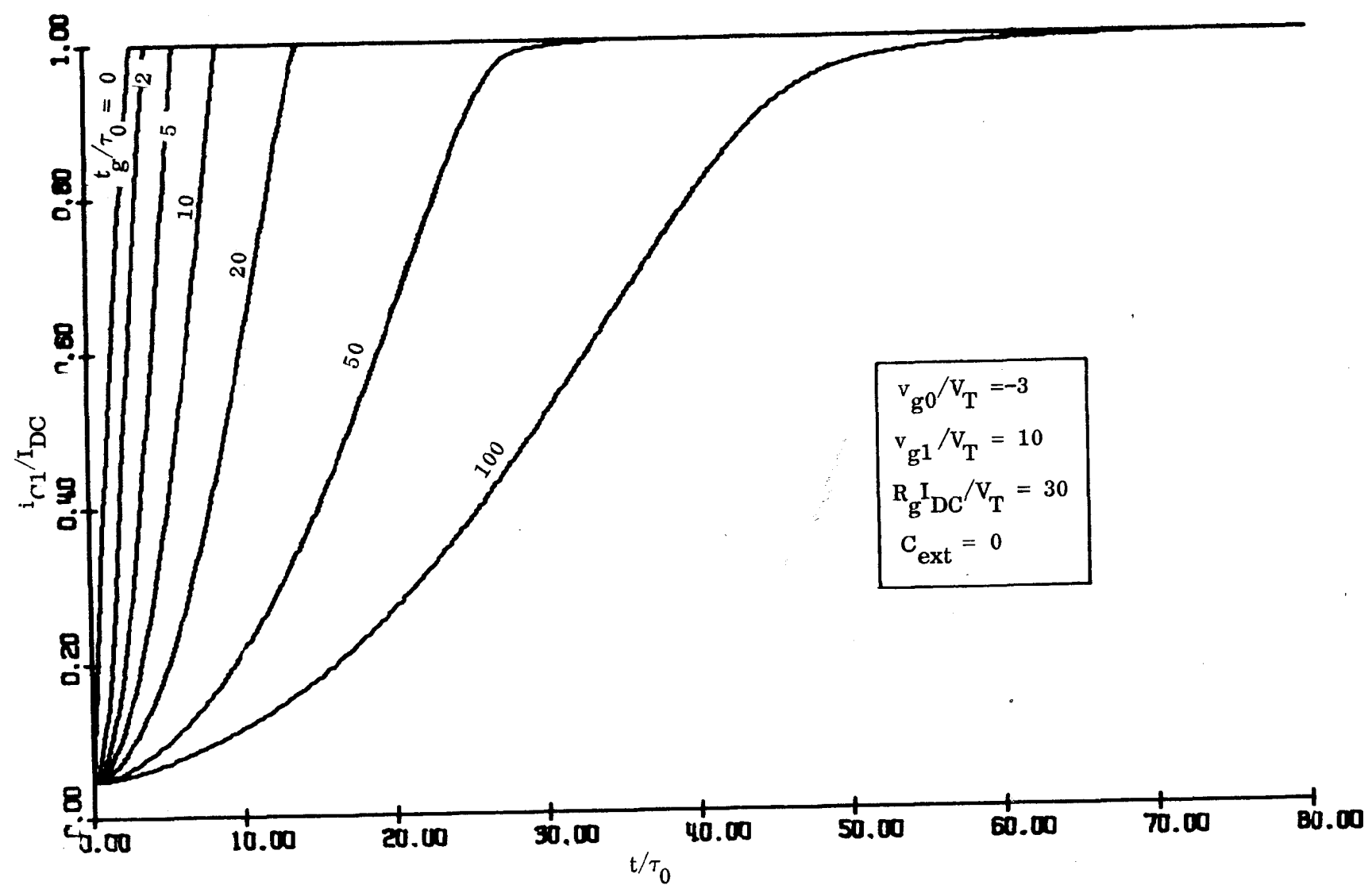


Fig. 8c

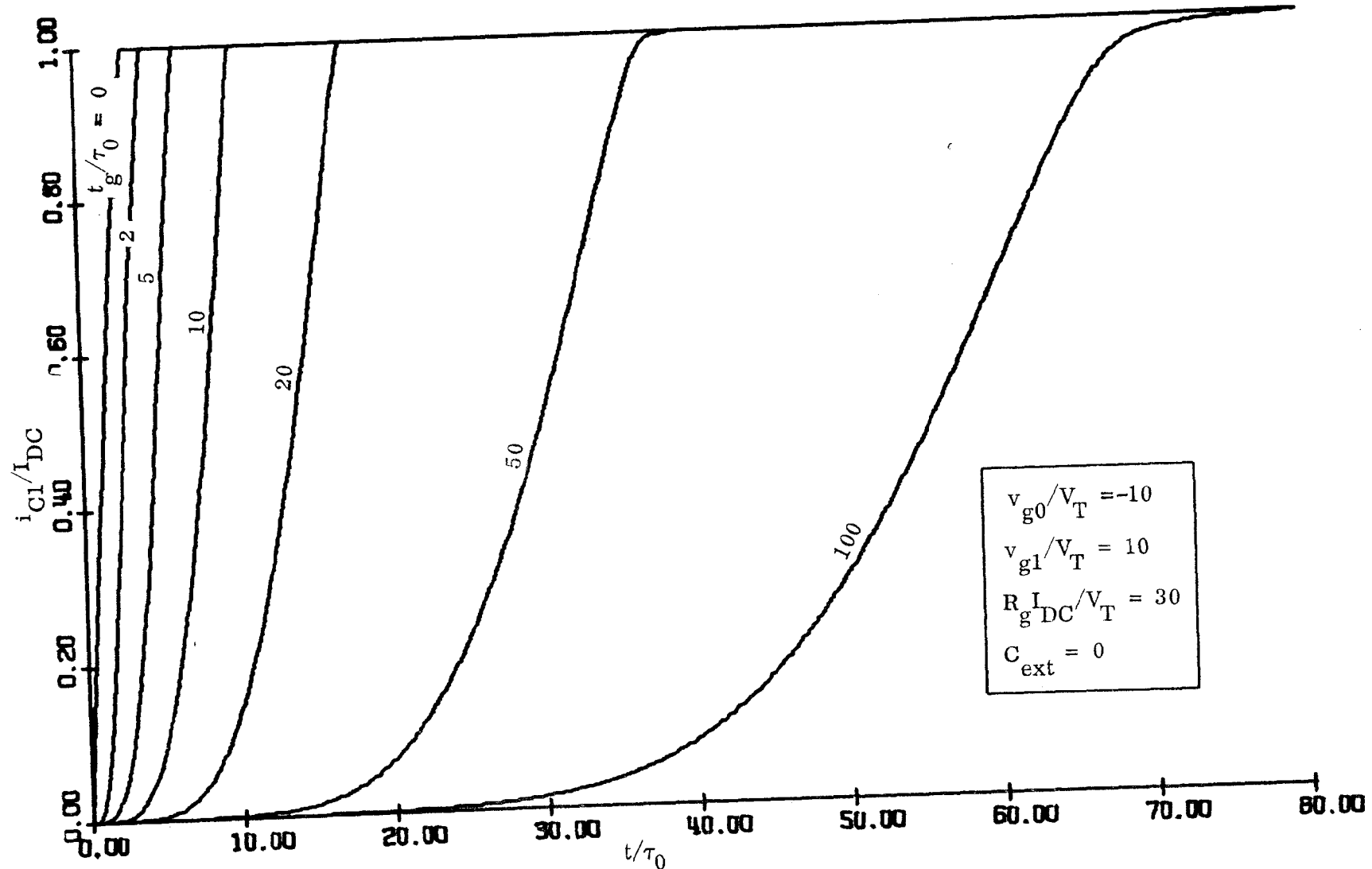


Fig. 8d

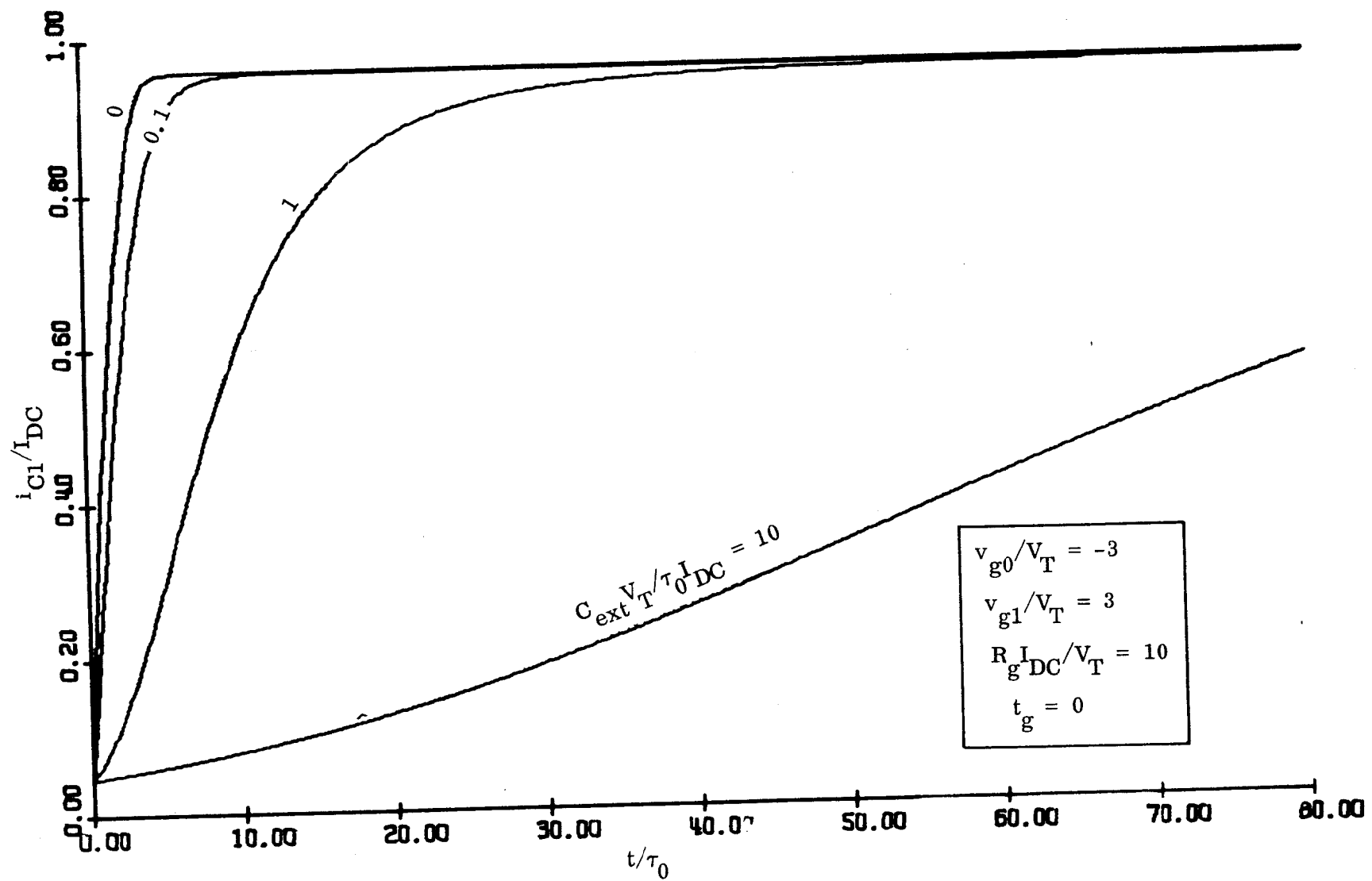


Fig. 9a

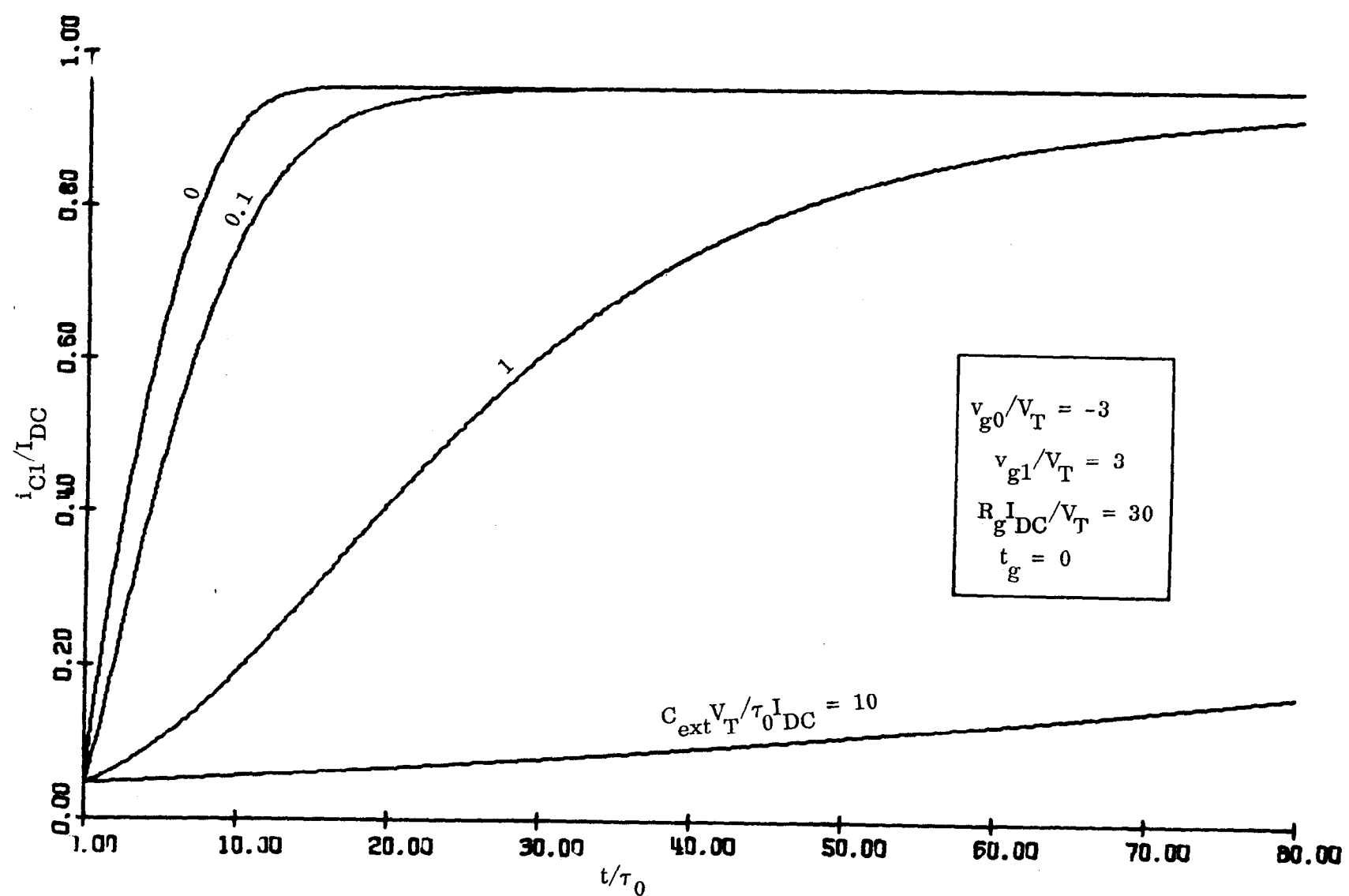


Fig. 9b

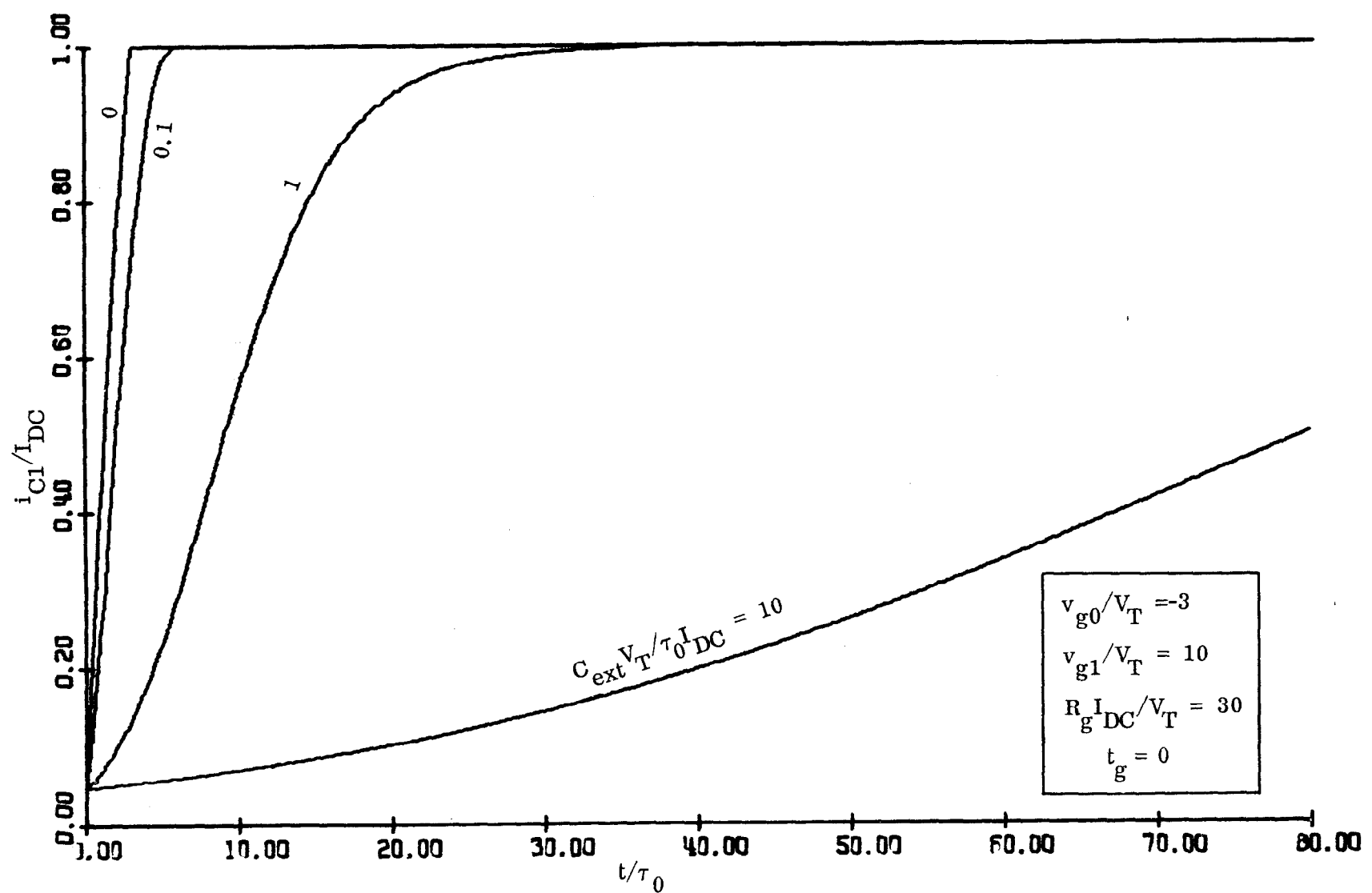


Fig. 9c

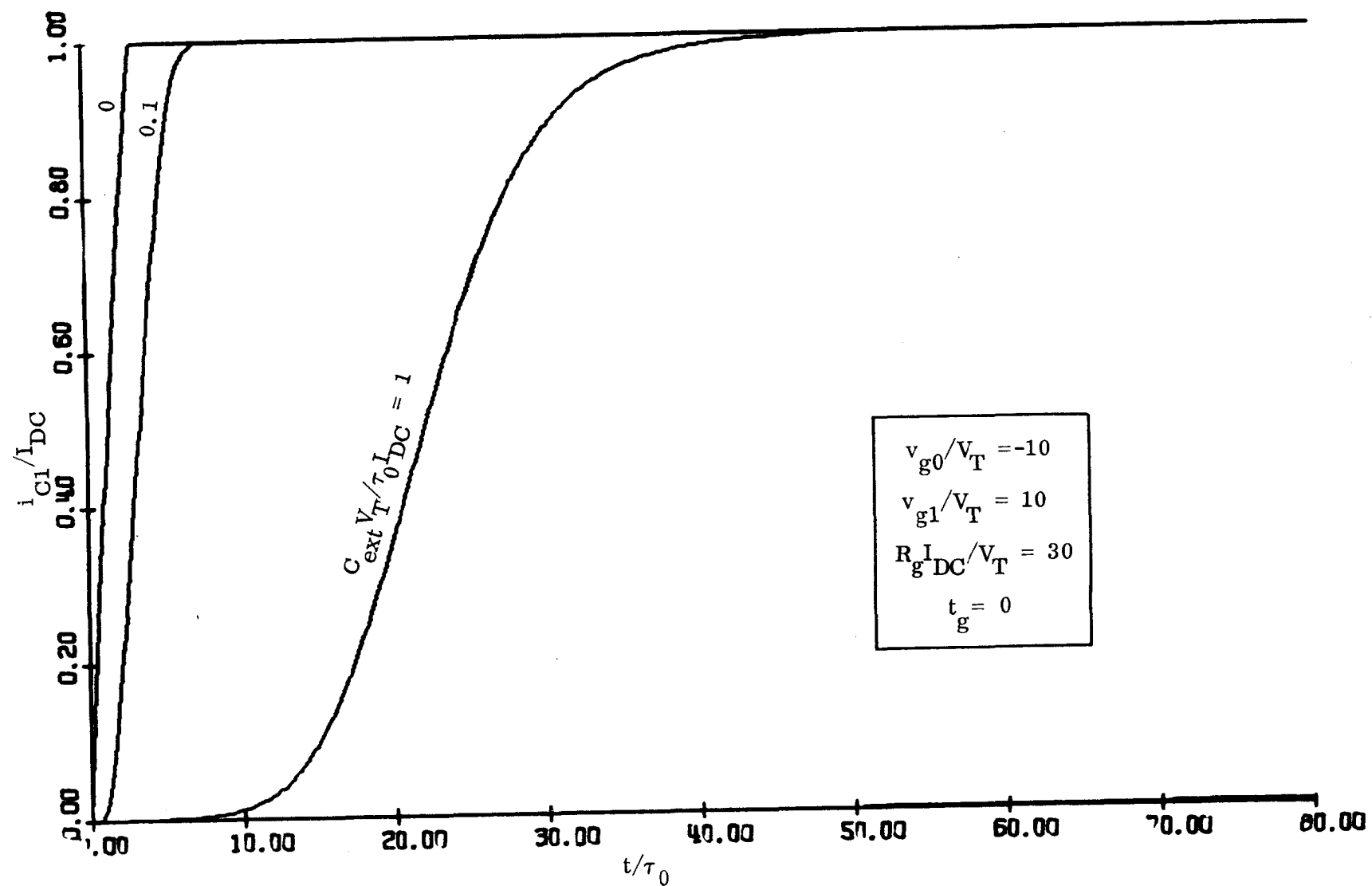


Fig. 9d